


RESEARCH

Open Access



A precise mathematical approach for analyzing the performance of MIMO space–time block code systems over Weibull fading channels

Abdelmajid Bessate^{1*} , Youssef Miftah^{2†}, Hussain Ben-Azza^{2†} and Faissal El Bouanani^{3†}

[†]Youssef Miftah, Hussain Ben-Azza and Faissal El Bouanani have contributed equally to this work.

*Correspondence:
bessate.a@ucd.ac.ma

¹ Polydisciplinary Faculty of Sidi Bennour, Chouaib Doukkali University, El Jadida, Morocco

² ENSAM, My Ismail University, Meknes, Morocco

³ Department of Embedded Systems, ENSIAS, Mohammed V University in Rabat, Rabat, Morocco

Abstract

Multiple-input–multiple-output (MIMO) systems have effectively addressed today's high demand for 5G communications and beyond. Further, MIMO-assisted space–time block codes (STBCs) have been shown to enhance the system's performance and provide a complete variety of coherent flat-fading channels. Additionally, the closed-form expression of the probability density function of the summation of correlated Weibull random variables remains unknown. In this work, we investigate the performance analysis of MIMO-STBC-enabled systems subject to the Weibull fading channel. New tight approximate expressions for numerous system performance metrics, e.g., outage probability, average capacity under various rate adaptation methods, and average symbol/bit error rate, have been obtained. The Monte Carlo simulation method has corroborated all the presented results.

Keywords: Average symbol error rate, Correlation, Moment-generating function, Multiple-input–multiple-output, Monte Carlo simulation method, Outage probability, Space–time block codes, Probability density function, Weibull distribution

1 Introduction

In response to the rising need for faster data speeds, multiple-input–multiple-output (MIMO) systems have become one of the most widely used wireless communication methods. Multiple antennas can be set up on both sides of the transmitter and receiver to increase system dependability. In addition, one of the pioneering aims realized with the usage of MIMO systems is to improve channel capacity without using up unnecessary frequency resources. Massive MIMO, in particular, has now become the key to transmission in wireless communications beyond 5G.

On the other hand, STBC (space–time block coding) [1] is a space–time conveying a diversity approach that allows the total system capacity to be increased. This approach was significantly enhanced in [2] to accommodate more than two transmit antennas using orthogonal STBC (OSTBC) models. Further, STBC codes have been shown to be effective in reducing the effects of fading and shadowing, as seen in [3].

Besides, the performance difference between non-ergodic STBC channel capacity and matrix MIMO channel capacity was investigated in [4]. In [5], the average symbol error rate (ASER) of STBCs with M -ary methods for modulation subject to fading channels with keyhole Nakagami- m was investigated in a closed form using the moment-generating function (MGF) technique. Average channel capacity and ASER of OSTBC for M -ary modulation schemes were investigated in [6], whereas the average STBC's average symbol error rate (ABER) was analyzed subject Rayleigh-correlated fading model in [7], and an upper bound was provided in [8–10]. Moreover, in [11], closed-form performance metrics for MIMO-STBC with generalized- K fading channels were found. Closed-form formulas for the average channel capacity (ACC) of MIMO-STBC experiencing Rayleigh fading channels were obtained, considering the effects of the receiver channel estimate errors, for several systems with adaptive transmissions in [12]. [13] investigated the ACC and ASER of STBCs for various modulation schemes and several fading models, but the symbol error rate was calculated for pulse-amplitude modulation (PAM), phase-shift keying (PSK), and quadrature amplitude modulation (QAM). The arbitrary fading distributions have been considered in [14], within the authors establish a broad, simple, and tight closed-form formula for the OP of MIMO-OSTBC systems.

On the other hand, the Weibull distribution is a valuable model and recently sparked a lot of interest in radio propagation in both indoor and outdoor environments. Also, it is commonly known that the expression of the PDF of the Weibull RVs' sum is not defined, even impossible to obtain a closed form. As an alternative way, multiple researchers have tried to present tight approximate expressions for such a PDF. In this direction, a PDF of MIMO systems was estimated in [15] using a finite mixture with an expectation-maximization approach over independent and identically distributed WFC. By the use of two new approximate expressions for the PDFs of Weibull's sum RVs [16, 17], the authors investigated the MIMO-STBC performance over independent and not necessarily identically distributed (i.n.i.d) Weibull fading channels (WFCs).

On the other hand, the authors in [18] have presented a tight approximation sum's PDF of altogether correlated Weibull RVs. Such an expression has been seen as the tightest one among the previous ones known in the literature. This is because the moment-based method employed in such a contribution used the five first moments of the distribution instead of less than three ones, utilized in other works. To this end, and leveraging this result, we present in this work accurate approximate expressions for various system's performance metrics, including the cumulative distribution function (CDF), OP, AC, and ASER is under-correlated and not necessarily identically distributed (c.n.i.d) Weibull RVs, whereas the correctness of these expressions has been checked using the Monte Carlo (MC) simulation method. The paper's remainder can be outlined as follows: The STBC system and channel design are presented in Sect. 2, while the statistical properties of MIMO-STBC in terms of tight approximation expressions are presented in Sect. 3. Section 4 illustrates the approximation's validation by depicting the figures of analytical expressions and simulating them using the MC approach. Finally, Sect. 5 concludes the work and points out some future directions.

2 Method

This study evaluates the performance criteria of MIMO system subject to Weibull fading Channels. However, the derivation of these performances is based on the probability density function (PDF) of the sum of received Weibull random variables. Since this pdf has not yet been derived analytically in a closed form, we divert this problem by adopting a tight approximate pdf in order to derive analytically the related expressions. The derived results are illustrated using Mathematica software and validated by the Monte Carlo simulation method.

3 System and channel design of MIMO-STBC

We explore a wireless communication system (WCS) founded on MIMO-STBC variety and working over c.n.i.d Weibull fading channels (WFC). In a general case, there are M_t and N_r antennas for the transmitter and receiver which compose the MIMO system. The transferred message contains R information bits, designed as symbols s_1, s_2, \dots, s_R and selected from the M -ary pleiad of signals with medium power ($P_S = E_s/M_t N_0$). Consequently, the symbols $\{S_i\}_{i=1}^R$ subject to a STBC encoding using $T \times M_t$ column orthogonal transfer matrix X

$$X = \begin{pmatrix} x_{ij} \\ i \leq M_t \\ j \leq T \end{pmatrix}, \tag{1}$$

where the entries x_{ij} act as a sleeve for the elements and conjugates of the signal constellation [5]. To send R symbols, we need T slots of time; hence, the pace of coding can be evaluated as follows

$$R_c = \frac{R}{T}. \tag{2}$$

The output of the channel for the n th input block covering T symbol periods is expressed at time nT , as shown in [19]

$$Y_{nT} = HX_{nT} + V_{nT}, \tag{3}$$

whether the signal that was received Y_{nT} is $N_r \times T$ matrix, fading channel H is $M_t \times N_r$ matrix, ciphered codeword X_{nT} is $M_t \times T$ matrix, and the received noise V_{nT} is $N_r \times T$ one. The fading channel $H = (h_{ij})$ is investigated as a matrix of Weibull with c.n.i.d circular complex Gaussian RVs. The i th receiving antenna's channel gain is mirrored with the j th transmitting antenna's channel gain by h_{ij} .

While the encoded matrix X_{nT} is created by combining ($R \leq T$) symbols that are ideal for code delay optimization. It goes without saying that not every M_t have a full rate ($R = T$) codes. Because of this, the R_c for STBC encoding is always ($R \leq T$)

Over flat channels of fading, the output SNR of a MIMO-STBC combiner can be stated as [20]

$$\gamma_s = \frac{E_s}{M_t R_c N_0} \|H\|_F^2, \tag{4}$$

whereabouts $\|H\|_F^2$ is the matrix H squared norm of Frobenius, E_s is the transmitter's average power per symbol, and N_0 is the Additive White Gaussian noise's power spectral density (AWGN). Applying the norm of Frobenius on the matrix H squared, we get

$$\gamma_s = \frac{1}{K} \sum_{i=1}^{M_t} \sum_{j=1}^{N_r} \gamma_{ij}, \tag{5}$$

whether $K = M_t R_c$ and γ_{ij} designates the instant SNR of each channel of fading presented in [21].

$$\gamma_{ij} = \frac{E_s}{N_0} |h_{ij}|^2 \tag{6}$$

The CDF of WFC gain $|h_{ij}|$ is derived by [22, e (3)] as

$$F_{|h_{ij}|}(r) = 1 - \exp\left[-\frac{r^\beta}{\Omega_{ij}}\right], \quad r \geq 0, \tag{7}$$

with Ω_{ij} is linked to the average power of fading $\mathbb{E}[|h_{ij}|^2]$ and the Gamma function [23] as

$$\Omega_{ij} = \left(\frac{\mathbb{E}[|h_{ij}|^2]}{\Gamma\left(1 + \frac{2}{\beta}\right)}\right)^{\frac{\beta}{2}}, \tag{8}$$

hence, its PDF is written as:

$$f_{|h_{ij}|}(r) = \frac{\beta r^{\beta-1}}{\Omega_{ij}} e^{-\frac{r^\beta}{\Omega_{ij}}}, \quad r \geq 0. \tag{9}$$

It can be seen that γ_{ij} is too a Weibull random variable (RV). Adopting (6) and (9), and following up with the Jacobian transform, the PDF of γ_{ij} can be expressed as

$$f_{\gamma_{ij}}(\gamma) = \frac{\beta \gamma^{\frac{\beta}{2}-1}}{2\omega_{ij}^{\frac{\beta}{2}}} \exp\left[-\left(\frac{\gamma}{\omega_{ij}}\right)^{\frac{\beta}{2}}\right], \tag{10}$$

where $\omega_{ij} = \frac{E_s}{N_0} \Omega_{ij}^{2/\beta}$ and $\frac{\beta}{2}$ represent the scale and shape parameters of γ_{ij} , respectively. It can be shown from (8) and (6) that

$$\omega_{ij} = \frac{\bar{\gamma}_{ij}}{\Gamma\left(1 + \frac{2}{\beta}\right)}. \tag{11}$$

4 Performance criteria

4.1 The total's PDF of c.n.i.d WFC

The relation between the maximal ratio combining (MRC) output SNR and the one of MIMO-STBC can be deduced from (5) as

$$\gamma_s = \frac{\gamma}{K}, \tag{12}$$

where $\gamma = \sum_{i=1}^{N_r} \sum_{j=1}^{M_t} \gamma_{ij}$ denotes the SNR (output) of $N_r \times M_t$ MRC receiver.

The PDF of the output SNR γ_s may be calculated using the equation above (12) and the new PDF of Weibull RVs described in [18, Eq. (2)], as well as the Jacobian transform.

$$f_{\gamma_s}(\gamma) \approx \lambda k G_{1,2}^{2,0} \left(\frac{K\gamma}{\theta} \middle| \begin{matrix} -; a_1 \\ b_1, b_2; - \end{matrix} \right), \tag{13}$$

where $G_{m,n}^{p,q} \left(\cdot \middle| \begin{matrix} \cdot \\ \cdot \\ \cdot \end{matrix} \right)$ shows the Meijer's G-function, and

$$\lambda = \frac{\Gamma(a_1 + 1)}{\theta \Gamma(b_1 + 1) \Gamma(b_2 + 1)}, \tag{14}$$

$$\theta = \frac{a_1}{2} (\varphi_4 - 2\varphi_3 + \varphi_2) + 2\varphi_4 - 3\varphi_3 + \varphi_2, \tag{15}$$

$$a_1 = \frac{4\varphi_4 - 9\varphi_3 + 6\varphi_2 - \mu_1}{-\varphi_4 + 3\varphi_3 - 3\varphi_2 + \mu_1}, \tag{16}$$

$$b_1 = \frac{c_1 + c_2}{2}, \tag{17}$$

$$b_2 = \frac{c_1 - c_2}{2}, \tag{18}$$

with

$$c_1 = \frac{a_1(\varphi_2 - \mu_1) + 2\varphi_2 - \mu_1}{\theta} - 3, \tag{19}$$

$$c_2 = \sqrt{\left(\frac{a_1(\varphi_2 - \mu_1) + 2\varphi_2 - \mu_1}{\theta} - 1 \right)^2 - 4 \frac{\mu_1(a_1 + 1)}{\theta}}, \tag{20}$$

$$\varphi_i = \frac{\mu_i}{\mu_{i-1}}, 1 \leq i \leq 4. \tag{21}$$

where μ_i is the i th moment of the RV X , and $\Gamma(\cdot)$ stand for the Gamma function [27, Eq. (6.1.1)].

4.1.1 Coefficients of correlation

Taking into account that the parameters of PDF $\lambda, a_1, \theta, b_1, b_2, c_1$ and c_2 are based on calculating of the moments μ_i , the correlation coefficient ρ_{ij}^{kl} between two RVs X_{ij} and Y_{kl} can appear in the computation of the expectation term $\mathbb{E}[X_{ij}Y_{kl}]$ as follows [18]

$$\rho_{ij}^{kl} = \frac{\frac{\mathbb{E}[X_{ij}Y_{kl}]}{\omega_{ij}\omega_{kl}} - d_1(\beta_{ij})d_1(\beta_{kl})}{\sqrt{(d_2(\beta_{ij}) - d_1^2(\beta_{ij}))(d_2(\beta_{kl}) - d_1^2(\beta_{kl}))}}, \tag{22}$$

where $d_k(x) = \Gamma(1 + k/x)$.

4.2 Moment-generating function (MGF)

The MGF is a metric function that, in addition to the PDF, may be used to assess the performance criteria of any WCS, particularly the ABER. The MGF may be calculated as

$$\mathcal{M}_\gamma(t) = \int_0^\infty \exp(-t\gamma)f_\gamma(\gamma)d\gamma, \tag{23}$$

where $f_\gamma(\gamma)$ is the PDF of variable γ .

Proposition 1 *The MGF of the MIMO-STBC output SNR γ_s over correlated WFC can be accurately approximated as follows:*

$$\mathcal{M}_{\gamma_s}(t) = \frac{\lambda k}{t} G_{2,2}^{2,1} \left(\frac{k}{\theta t} \middle| \begin{matrix} 0; a_1 \\ b_1, b_2; - \end{matrix} \right) \tag{24}$$

Proof Rewriting the exponential function in (23) by Meijer G -Function based on the reference ([26, /07.34.03.0228.01]) and replacing the PDF expression (13) into above expression (23) can be stated as a product of two Meijer G -Function factors as

$$\mathcal{M}_{\gamma_s}(t) = \lambda K \int_0^\infty \gamma^{\alpha-1} G_{1,2}^{2,0}(t\gamma|0) G_{1,2}^{2,0} \left(\frac{K\gamma}{\theta} \middle| \begin{matrix} -; a_1 \\ b_1, b_2; - \end{matrix} \right) d\gamma \tag{25}$$

with $\alpha = 1$. Based on the reference ([26, /07.34.21.0011.01]), and manipulating some algebraic operations, the MGF expression (24) can be easily obtained. \square

4.3 The outage probability of output SNR

The OP of a WC system is the primary parameter used to calculate the output SNR. The CDF of a minimal output SNR, can be given as

$$P_{\text{out}} = F_\gamma(\gamma_{\text{th}}). \tag{26}$$

Proceeding by the CDF of c.n.i.d Weibull RVs derived in [18, Eq. (31)] and recalling the Jacobi transform, the approximate expression for the OP of MIMO-STBC subject to c.n.i.d WFC can be obtained as

$$P_{\text{out}} \approx \lambda \theta K G_{2,3}^{2,1} \left(\frac{K\gamma_{\text{th}}}{\theta} \middle| \begin{matrix} 1; a_1 + 1 \\ b_1 + 1, b_2 + 1; 0 \end{matrix} \right). \tag{27}$$

4.4 Average symbol error probability (ASEP)

Proposition 2 *The ASEP for most various M-ary modulation schemes with MIMO-STBC coding over c.n.i.d WCF can be approximated with accuracy by*

$$\bar{P}_s \approx \frac{\lambda K \varrho}{\delta \sqrt{\pi}} G_{3,3}^{2,2} \left(\frac{K}{\theta \delta} \middle| \begin{matrix} 0, -\frac{1}{2}; a_1 \\ b_1, b_2, -1; - \end{matrix} \right), \tag{28}$$

where ϱ and δ are two parameters corresponding to the modulation policy [9, Table I].

Proof The ASEP for various M-ary modulation policies is expressed over fading channel as

$$\bar{P}_s = \int_0^{+\infty} P_{se}(\gamma) f_{\gamma_s}(\gamma) d\gamma, \tag{29}$$

where the instantaneous ASEP $P_{se}(\gamma)$ can be expressed in terms of the complementary error function as

$$P_{se}(\gamma) = \varrho \operatorname{erfc}(\sqrt{\delta \gamma}). \tag{30}$$

Now, by replacing (13) and (30) into (29) with the use of [26, /06.27.26.0006.01], the approximate ASEP changes into

$$\bar{P}_s \approx \frac{\lambda K \varrho}{\sqrt{\pi}} \int_0^{+\infty} G_{1,2}^{2,0} \left(\delta \gamma \middle| \begin{matrix} 1 \\ 0, \frac{1}{2} \end{matrix} \right) G_{1,2}^{2,0} \left(\frac{K \gamma}{\theta} \middle| \begin{matrix} -, a_1 \\ b_1, b_2 \end{matrix} \right) d\gamma. \tag{31}$$

Based on [26, /07.34.21.0012.01], the formula in (28) can readily be derived, which brings the proof to a close. □

4.5 Average bit error rate (ABER)

The ABER can be computed as ([24, Eq. (19)])

$$\bar{P}_e = \frac{\varrho}{\pi} \int_0^{\frac{\pi}{2}} M_{\gamma_s} \left(\frac{\delta}{\sin^2(\phi)} \right) d\phi, \tag{32}$$

where $M_{\gamma_s}(\cdot)$ is the MGF of the MIMO-STBC output SNR.

Proposition 3 *The ABER of the MIMO-STBC output SNR γ_s over correlated WFC can be accurately approximated as*

$$\bar{P}_e = \frac{\lambda k \varrho}{2 \delta \sqrt{\pi}} G_{3,3}^{2,2} \left(\frac{k}{\delta \theta} \middle| \begin{matrix} 0, -\frac{1}{2}; a_1 \\ b_1, b_2; -1 \end{matrix} \right). \tag{33}$$

Proof Substituting the MGF expression (24) into (32) after rewriting it by its Mellin–Barnes form, the expression in (32) can be rewritten as

$$\bar{P}_e = \frac{\lambda k_Q}{\delta \pi} \frac{1}{2\pi j} \int_c \frac{\Gamma(b_1 + s)\Gamma(b_2 + s)\Gamma(1 - s)}{\Gamma(a_1 + s)} \left(\frac{k}{\delta \theta}\right)^{-s} Ids \tag{34}$$

The term $I = \int_0^{\frac{\pi}{2}} \sin^{2-2s}(\phi) d\phi$ can be rewritten as $\int_0^{\frac{\pi}{2}} \sin^{2(\frac{3}{2}-s)-1}(\phi) \cos^{2\frac{1}{2}-1}(\phi) d\phi$ which is obvious equal $\frac{1}{2}B(\frac{3}{2} - s, \frac{1}{2})$, with $B(., .)$ is the Beta function. Rewriting the Beta function in terms of Gamma function, we obtain

$$B\left(\frac{3}{2} - s, \frac{1}{2}\right) = \frac{\sqrt{\pi}\Gamma\left(\frac{3}{2} - s\right)}{\Gamma(2 - s)} \tag{35}$$

□

Finally, replacing (35) into (34), Eq. (33) can be readily obtained.

4.6 Average capacity under ORA scheme

Proposition 4 Under optimal rate adaptation (ORA) scheme, an average channel capacity (ACC) can be very closely approximated as:

$$\bar{C} \approx \frac{\lambda K R_c B_w}{\ln 2} G_{3,4}^{4,1} \left(\frac{K}{\theta} \middle| \begin{matrix} -1; a_1, 0 \\ b_1, b_2, -1, -1; - \end{matrix} \right). \tag{36}$$

taken that B_w is the channel bandwidth.

Proof For a flatness fading channel, the ACC can be expressed as [12, Eq. (15)]

$$\bar{C} = R_c B_w \mathbb{E}[\log_2(1 + \gamma_s)] = R_c B_w \int_0^{+\infty} \log_2(1 + \gamma_s) f_{\gamma_s}(\gamma) d\gamma \tag{37}$$

with

$$\mathbb{E}[\log_2(1 + \gamma_s)] = \int_0^{+\infty} \log_2(1 + \gamma_s) f_{\gamma_s}(\gamma) d\gamma$$

□

In the same way as the ASER computation and substituting (13) and using [26, /07.34.03.0456.01] into 37, we get:

Proof

$$\bar{C} \approx \lambda K R_c B_w \int_0^{+\infty} M2 d\gamma. \tag{38}$$

with

$$M2 = G_{2,2}^{1,2} \left(\gamma_s \middle| \begin{matrix} 1, 1; - \\ 1; 0 \end{matrix} \right) G_{1,2}^{2,0} \left(\frac{K\gamma}{\theta} \middle| \begin{matrix} -; a_1 \\ b_1, b_2; - \end{matrix} \right)$$

□

By applying the result mentioned in [26, /07.34.21.0012.01] on (38), we get (36), which concludes the proof.

4.7 Average capacity under OPRA policy

The OPRA channel capacity is given by [12, Eq. (26)]

$$\bar{C}_{\text{opra}} = R_c B_w \int_{\gamma_0}^{+\infty} \log_2 \left(\frac{\gamma}{\gamma^*} \right) f_\gamma(\gamma) d\gamma, \tag{39}$$

where γ^* is the SNR of optimal cutoff under it no data are transmitted, i.e, [25, Eq. (6)]

$$\int_{\gamma_0}^{+\infty} \left(\frac{1}{\gamma^*} - \frac{1}{\gamma} \right) f_\gamma(\gamma) d\gamma = 1 \tag{40}$$

Proposition 5 *The average OPRA capacity of MIMO-STBC over correlated WFC can be accurately approximated by:*

$$\bar{C}_{\text{opra}} = \frac{\gamma^* R_c B_w \lambda k}{\ln 2} G_2, \tag{41}$$

with

$$G_2 = G_{0,1:2,1:2,2}^{1,0:1,2:2,0} \left(1, \frac{k\gamma^*}{\theta} \middle| \begin{matrix} -; - & : & 1, 1; - & : & -; a_1, 0 \\ 1; - & : & 1; - & : & b_1, b_2; - \end{matrix} \right).$$

where G_{\dots} stands for the Bivariate Meijer's G-function expression in [12].

Proof Based on [26, /07.34.03.0456.01] and replacing (13) into (39), the OPRA capacity can be computed as:

$$\bar{C}_{\text{opra}} = \frac{R_c B_w \lambda k}{\ln 2} \int_{\gamma^*}^{+\infty} 2G d\gamma$$

with

$$2G = G_{2,2}^{1,2} \left(\frac{\gamma}{\gamma^*} - 1 \middle| \begin{matrix} 1, 1 \\ 1, 0 \end{matrix} \right) G_{1,2}^{2,0} \left(\frac{K\gamma}{\theta} \middle| \begin{matrix} -; a_1 \\ b_1, b_2; - \end{matrix} \right)$$

□

Replacing the two Meijer G-Functions by their Mellin–Barnes forms, (41) can be rewritten as:

$$\bar{C}_{\text{opra}} = \frac{R_c B_w \lambda k}{\ln 2} \frac{1}{(2\pi j)^2} 2L \underbrace{\int_{\gamma_0}^{+\infty} \left(\frac{\gamma}{\gamma^*} - 1 \right)^{-s} \left(\frac{k}{\theta} \gamma \right)^{-t} d\gamma}_I \tag{42}$$

with

$$2L = \int_{\mathcal{L}_1} \int_{\mathcal{L}_2} \frac{\Gamma(s+1)\Gamma^2(-s)}{\Gamma(1-s)} \frac{\Gamma(b_1+t)\Gamma(b_2+t)}{\Gamma(a_1+t)} dsdt$$

Using the change of variable $x = \frac{\gamma_0}{\gamma}$ and performing some algebraic operations, \mathcal{I} can be written as, for $\Re(s) < 1$ and $\Re(s+t) > 1$

$$\mathcal{I} = \gamma^* \left(\frac{k}{\theta} \gamma^*\right)^{-t} \int_0^1 (1-x)^{-s} x^{s+t-2} dx \tag{43}$$

Rewriting the Beta function in terms of product of Gamma functions yields

$$\begin{aligned} \mathcal{I} &= \gamma^* \left(\frac{k}{\theta} \gamma^*\right)^{-t} B(s+t-1, 1-s) \\ &= \gamma^* \left(\frac{k}{\theta} \gamma^*\right)^{-t} \frac{\Gamma(s+t-1)\Gamma(1-s)}{\Gamma(t)}. \end{aligned} \tag{44}$$

Now, substituting (44) into (42), the expression (42) becomes

$$\bar{C}_{\text{opra}} = \gamma^* \frac{R_c B_w \lambda k}{\ln 2} \frac{1}{(2\pi j)^2} \int_{\mathcal{L}_1} \int_{\mathcal{L}_2} \Gamma_{st} \times \left(\frac{k}{\theta} \gamma^*\right)^{-t} dsdt, \tag{45}$$

with

$$\Gamma_{st} = \frac{\Gamma(s+t+1)\Gamma(s+1)\Gamma^2(-s)\Gamma(b_1+t)\Gamma(b_2+t)}{\Gamma(t)\Gamma(a_1+t)}.$$

Consequently, (41) is attained, which brings the proof to a close.

4.7.1 Optimal cutoff SNR γ^*

The optimal cutoff level, under it the transfer of data is halted, must verify (40). As no data are transmitted when $\gamma < \gamma^*$, the optimal policy goes through an OP P_{out} , match the probability of cutoff, provided by

$$P_{\text{out}} = 1 - \int_{\gamma^*}^{+\infty} f_{\gamma}(\gamma) d\gamma. \tag{46}$$

(40) can be rewritten as:

$$p(\gamma_0) = \frac{1}{\gamma^*} F_{\gamma}^c(\gamma_0) d\gamma - \int_{\gamma^*}^{\infty} \frac{1}{\gamma} f_{\gamma}(\gamma) d\gamma - 1. \tag{47}$$

To prove the uniqueness of the solution γ^* , we have to prove the monotony of function $p(\cdot)$ and further evaluate its limits at 0 and infinity. For all types of fading distributions, the derivative of the above function can be written as:

$$p'(\gamma^*) = \left(\frac{1}{\gamma^*} F_{\gamma}^c(\gamma^*) d\gamma\right)' - \frac{\partial \left[\int_{\gamma^*}^{\infty} \frac{1}{\gamma} f_{\gamma}(\gamma) d\gamma\right]}{\partial \gamma^*}. \tag{48}$$

Moreover,

$$\left(\frac{1}{\gamma^*} F_{\gamma}^c(\gamma_0) d\gamma\right)' = -\frac{1}{(\gamma^*)^2} F_{\gamma}^c(\gamma^*) d\gamma - \frac{f_{\gamma}(\gamma^*)}{\gamma^*}, \tag{49}$$

and

$$\frac{\partial \left[\int_{\gamma^*}^{\infty} \frac{1}{\gamma} f_{\gamma}(\gamma) d\gamma \right]}{\partial \gamma^*} = -\frac{f_{\gamma}(\gamma^*)}{\gamma^*}. \tag{50}$$

Thus,

$$p'(\gamma^*) = -\frac{1}{(\gamma^*)^2} F_{\gamma}^c(\gamma^*) < 0, \tag{51}$$

as

$$\begin{aligned} \lim_{\gamma^* \rightarrow 0} p(\gamma^*) &= \lim_{\gamma^* \rightarrow 0} \underbrace{\frac{1}{\gamma^*} F_{\gamma}^c(\gamma^*)}_{=\infty} - \underbrace{\mathbb{E}_{\gamma} [\gamma^{-1}]}_{\text{Finite Term}} - 1 \\ &= \infty, \end{aligned} \tag{52}$$

and

$$\begin{aligned} \lim_{\gamma^* \rightarrow \infty} p(\gamma^*) &= \lim_{\gamma^* \rightarrow \infty} \underbrace{\frac{1}{\gamma^*} F_{\gamma}^c(\gamma^*)}_{=0} - \underbrace{\int_{\gamma^*}^{\infty} \frac{1}{\gamma} f_{\gamma}(\gamma) d\gamma}_{=0} - 1 \\ &= -1. \end{aligned} \tag{53}$$

Finally, taking into consideration the obtained limits and monotony of $p'(\gamma^*)$ proved in (51), we conclude that the optimal cutoff SNR γ^* exists and is unique.

4.8 Average capacity under CIFR policy

The channel capacity of MIMO-STBC using a CIFR policy is given by [12, Eq. (44)]:

$$\bar{C}_{\text{cifr}} = R_c B_w \log_2 \left(1 + \frac{1}{\int_0^{\infty} \gamma^{-1} f_{\gamma}(\gamma) d\gamma} \right). \tag{54}$$

Proposition 6 *The ACC of MIMO-STBC, employing CIFR policy, experiencing a correlated WF can be tightly approximated by:*

$$\bar{C}_{\text{cifr}} = R_c B_w \log_2 \left(1 + \frac{\Gamma(a_1)}{\lambda K \Gamma(b_1) \Gamma(b_2)} \right) \tag{55}$$

where the parameters a_1 , b_1 and b_2 are expressed in the first subsection above, and $\Gamma(\cdot)$ denotes the Gamma function.

Proof The integral $\int_0^{\infty} \gamma^{-1} f_{\gamma}(\gamma) d\gamma$ can be expressed, after replacing the PDF (13), as

$$\mathcal{I} = \lambda K \int_0^{\infty} \gamma^{-1} G_{1,2}^{2,0} \left(\frac{K\gamma}{\theta} \middle| \begin{matrix} -; a_1 \\ b_1, b_2; - \end{matrix} \right) d\gamma. \tag{56}$$

Based on the identity in the reference [26, /07.34.21.0009.01], the integral I can be expressed as:

$$\mathcal{I} = \frac{\lambda K \Gamma(b_1) \Gamma(b_2)}{\Gamma(a_1)} \tag{57}$$

Replacing the expression (57) into (54), the equation in (55) can be obtained. \square

4.9 Average capacity under TCIFR policy

The TCIFR capacity can be computed as:

$$\bar{C}_{tcifr} = R_c B_w \log_2 \left[1 + \frac{1}{\int_{\gamma_0}^{\infty} \gamma^{-1} f_{\gamma}(\gamma) d\gamma} \right] (1 - P_{out}(\gamma_0)). \tag{58}$$

Proposition 7 *The ACC metric, employing TCIFR policy, for the correlated MIMO-STBC output SNR experiencing a Weibull fading can expressed as follows:*

$$\bar{C}_{tcifr} = R_c B_w \log_2 (\mathcal{J} \times \mathcal{K}), \tag{59}$$

with

$$\mathcal{J} = 1 + \frac{1}{\lambda K G_{2,0}^{3,0} \left(\frac{K\gamma_0}{\theta} \middle| \begin{matrix} -; a_1, 1 \\ b_1, b_2, 0; - \end{matrix} \right)}, \tag{60}$$

and

$$\mathcal{K} = 1 - \lambda \theta K G_{2,3}^{2,1} \left(\frac{K\gamma_0}{\theta} \middle| \begin{matrix} 1; a_1 + 1 \\ b_1 + 1, b_2 + 1; 0 \end{matrix} \right). \tag{61}$$

Proof Rewriting the PDF function in (13) by its Mellin–Barnes form, the integral $I = \int_{\gamma_0}^{\infty} \gamma^{-1} f_{\gamma}(\gamma) d\gamma$ can be expressed as follows:

$$\mathcal{J} = \frac{\lambda K}{2\pi i} \int_c \frac{\Gamma(b_1 + s) \Gamma(b_2 + s)}{\Gamma(a_1 + s)} \left(\frac{K}{\theta} \right)^{-s} ds \int_{\gamma_0}^{\infty} \gamma^{-s-1} d\gamma. \tag{62}$$

By using the identity $\Gamma(s + 1) = s\Gamma(s)$, the integral I can be written as:

$$\mathcal{J} = \frac{\lambda K}{2\pi i} \int_c \frac{\Gamma(b_1 + s) \Gamma(b_2 + s) \Gamma(s)}{\Gamma(a_1 + s) \Gamma(s + 1)} \left(\frac{K}{\theta} \gamma_0 \right)^{-s} ds. \tag{63}$$

Now, it is obvious that I is nothing but a Mellin–Barnes integral corresponding to the following Meijer’s G-function

$$\mathcal{J} = \lambda K G_{2,0}^{3,0} \left(\frac{K\gamma_0}{\theta} \middle| \begin{matrix} -; a_1, 1 \\ b_1, b_2, 0; - \end{matrix} \right). \tag{64}$$

Substituting (64) and (27) into (58), we get (59). This brings the proposition’s proof to a close. \square

5 Results and discussion

5.1 Figures

This part contains several analytical results, which are illustrated to demonstrate the preciseness of the suggested approximate PDF on the performance metrics of MIMO-STBC. These performances, including PDF, OP, ASER, and ACC, are assessed by Mathematica software. Furthermore, the tightness of the convergent CDF is checked by the use of the Kolmogorov-Sprocess, and Figure 2 manifests good outcomes. Otherwise, the approximate PDF and the rest of the outcomes are proved by the Monte Carlo method using (5) by producing $M_t \times N_r \times 10^7$ Weibull-distributed random values. For all figures, the R_c value is taken equal to 0.5 except figure 9 and the β_{ij} value is supposed to be the same for each channel of transmission, while the parameter ω_{ij} is chosen =1.

Figure 1 illustrates both PDFs (i.e., analytical and simulated) of the output SNR versus γ_s for 2×3 MIMO-STBC encoding. The PDF figure is drawn from (13) for correlated RVs with ($\rho = 0.9$) and independent ones ($\rho = 0$). Besides, in a simulation way, the SNR range $[0, 13]$ is split up into 130 sub-intervals of equal length. By comparing the analytical PDFs and the feigned ones, it is obvious that they are very close to each other, which demonstrates the preciseness of this approach. Moreover, it can be shown from the correlated curvature and the uncorrelated ones that the correlation decreases the likelihood of achieving an output SNR.

Figure 2 represents two numerical results that of the CDF (γ_{th}) (outage probability) and that of EDF (empirical distribution function) of 2×3 MIMO-STBC system, for correlated RVs ($\rho = 0.9$) and independent ones ($\rho = 0$) with various values of β ($\beta = 1$ and $\beta = 2.5$). It is obvious from this figure that the correlation has a negative impact on achieving an output SNR, and the accuracy of this approximation appears evident based on the simulation.

Figure 3 presents both simulation and approximation of MGF expressed in (24). These results are illustrated versus t for jointly correlated RVs ($\rho = 0.9$) and independent ones ($\rho = 0$) under 2×3 MIMO-STBC system over c.n.i.d WFC. What is evident from this figure is that the analytical and simulated results are identical, which shows the high precision of our approach and adds another to derive the performance

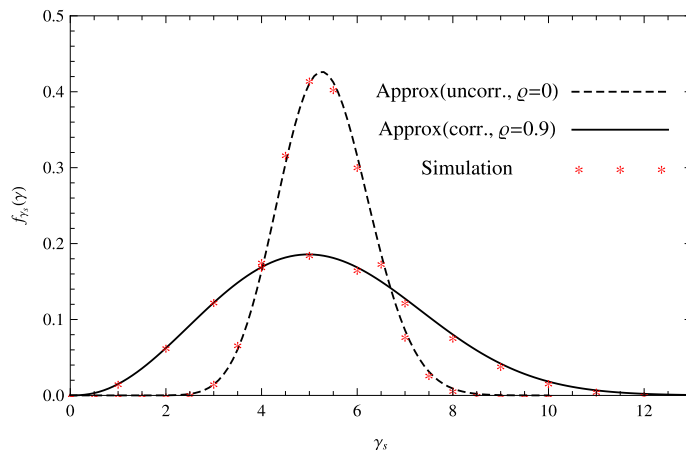


Fig. 1 PDF of the MIMO-STBC output SNR

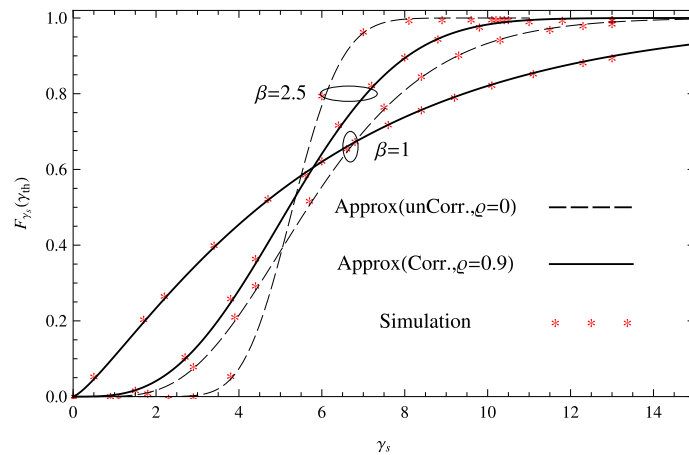


Fig. 2 CDF of 2×3 MIMO-STBC output SNR

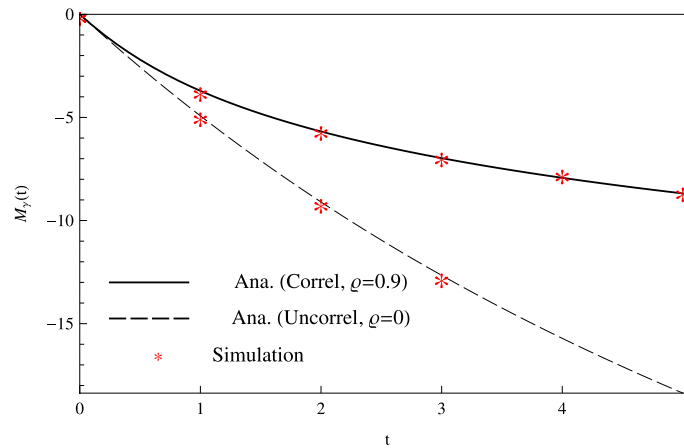


Fig. 3 MGF of correlated 2×3 MIMO-STBC output SNR

criteria. In addition, correlation diverges the MGF of MIMO-STBC in comparison with the independent case.

Figure 4 deals with the approximate and the simulated ASER mentioned in (28). The numerical results are drawn versus N_r for correlated RVs ($\rho = 0.9$) and independent ones ($\rho = 0$) with a fixed value of β ($\beta = 2.5$) under B -PSK modulation policies for $2 \times N_r$ MIMO-STBC system over c.n.i.d WFC. What is evident from this figure is that the correlation reduces the achievement of MIMO-STBC in comparison with the independent case. Furthermore, as the number of receiver antennas rises the likelihood to receive a symbol in error reduces which proves the usefulness of that system.

Figure 5 stands for the simulation and approximation of ABER given in (33). The numerical results are drawn versus N_r for jointly correlated RVs ($\rho = 0.9$) and independent ones ($\rho = 0$) with a fixed value of β ($\beta = 2.5$) under B -PSK modulation policies for $2 \times N_r$ MIMO-STBC system with c.n.i.d WFC. What is obvious from this figure is that the correlation phenomenon reduces the performance of MIMO-STBC

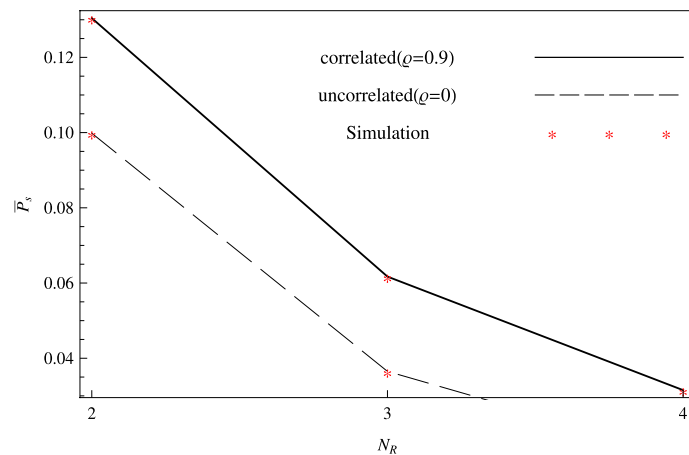


Fig. 4 ASER for BPSK modulation scheme

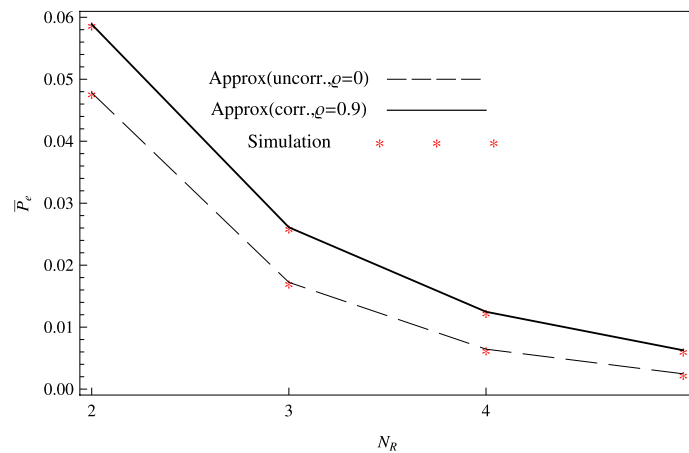


Fig. 5 ABER of correlated MIMO-STBC system

in comparison with the uncorrelated case. Moreover, the number of receiver antennas is higher, and the likelihood to receive a wrong bit is lower.

Figure 6 depicts the analytical and simulated ORA capacities versus N_r of MIMO-STBC combiner, illustrated, respectively, from (36), and via simulation from (37), for two cases, correlated RVs ($\rho = 0.9$) and independent ones ($\rho = 0$) with fixed values of $\beta = 3$ and $R_c = 0.5$. The effect of the correlation phenomenon on capacity is obvious by reducing it. Besides, the analytical and simulated ORA capacities are confused, which demonstrates the precision of that result. In the end, the bigger the number of N_r is, the bigger AC is, which manifests the utility of the MIMO-STBC. Table 1 shows more numerical results of capacity for various numbers of transmitters.

Figure 7 plots simulated and approximate capacity under CIFR policy given in (55). The numerical results are drawn versus N_r for two cases correlated RVs ($\rho = 0.9$) and independent ones ($\rho = 0$) with a fixed $R_c = 0.5$ for $2 \times N_r$ MIMO-STBC system upon correlated and identically distributed WFC. What is evident from these curves is that the correlation phenomenon decreases the capacity of MIMO-STBC in comparison with

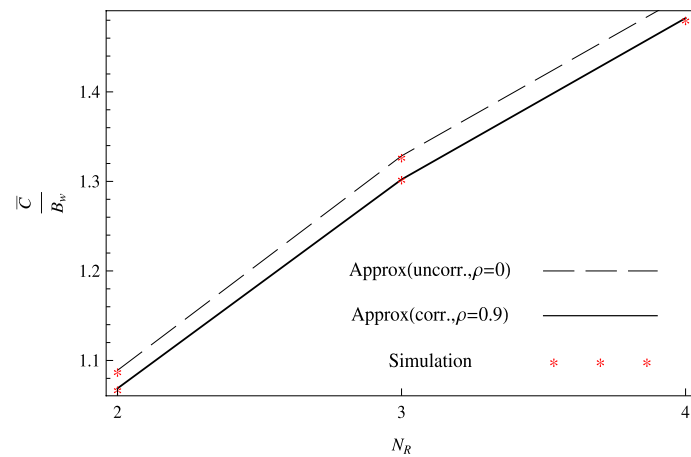


Fig. 6 ORA capacity of $2 \times N_r$ MIMO-STBC

Table 1 Capacity values for various numbers of transmitter/receivers

Capacity/ $M_t \times N_r$	2×2	2×3	2×4	3×3	4×4
Analytical value	1.06881	1.30216	1.48236	1.24988	1.48177
Simulated value	1.068796	1.303862	1.481745	1.251259	1.488821

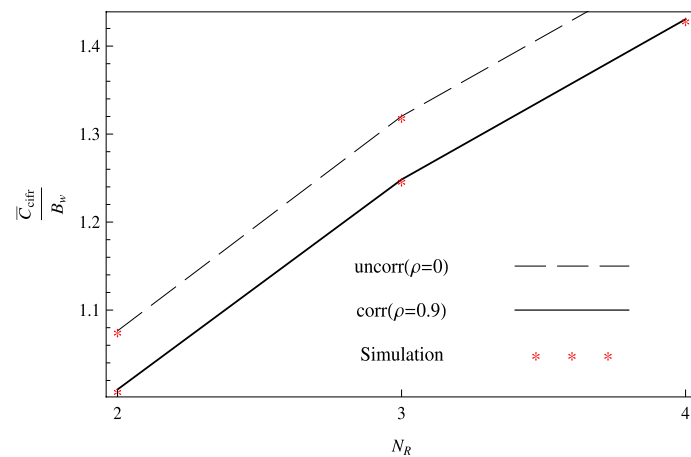


Fig. 7 CIFR capacity of $2 \times N_r$ MIMO-STBC

the independent case. Moreover, the number of receiving antennas rises as the capacity rises.

Figure 8 illustrates simulated and approximate TCIFR capacity given in (58) and (59), respectively. The numerical results are drawn versus N_r for two cases correlated RVs ($\rho = 0.9$) and independent ones ($\rho = 0$) with a fixed fade depth $\gamma_0 = 0.5$ and a code rate $R_c = 0.5$ for $2 \times N_r$ MIMO-STBC system over c.n.i.d WFC. It can be seen from the curves that correlation reduces the capacity of MIMO-STBC in comparison with the independent case. Furthermore, the higher the number of receiver antennas is, the greater the capacity is.

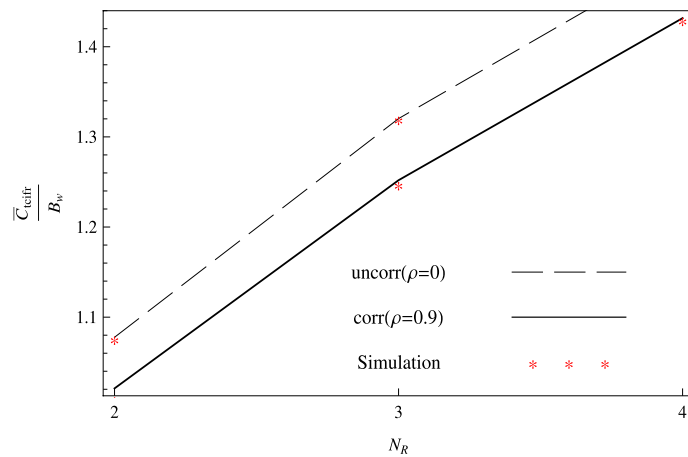


Fig. 8 TCIFR capacity of 2 × N_r MIMO-STBC

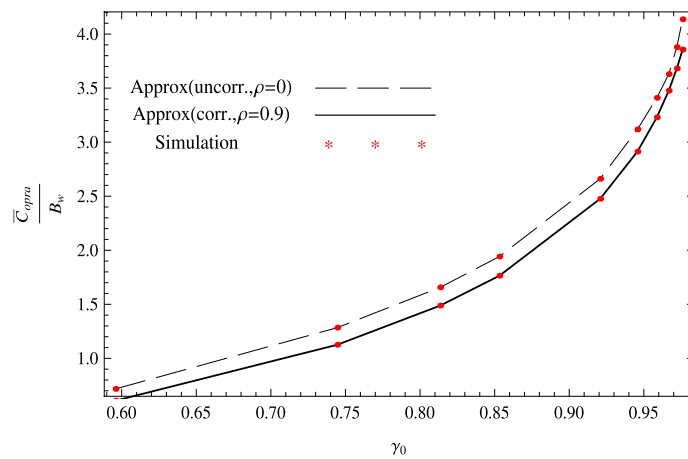


Fig. 9 OPRA capacity of 2 × N_r MIMO-STBC

Figure 9 shows simulated and approximate capacity under OPRA adaptation scheme, which are mentioned in (39) and (41), respectively. The curves are plotted versus the optimal cutoff γ^* for two correlated RV cases ($\rho = 0.9$) and independent ones ($\rho = 0$) with a code rate $R_c = 0.8$ for 2 × 3 MIMO-STBC system over c.n.i.d WFC. What is obvious from the drawn curves is the negative effect of correlation over the capacity of MIMO-STBC. In addition, as γ^* increases, the capacity increases.

5.2 Complexity

Table 2 shows the complexity in terms of consumed time to evaluate each obtained result either analytical or simulated. The evaluation was done by a laptop with the following features:

- **Processor:** 11th Gen Intel(R) Core(TM) i5-1135G7 @ 2.40GHz 2.42 GHz
- **Memory:** 16 Go

Table 2 Time complexity of analytical and simulated results

Result/time (s)	Analytical method	Simulated method
ASER	0.0138659	≈ 50
ABER	0.0129678	≈ 50
ORA Capacity	0.031250	≈ 50
OPRA Capacity	0.029571	≈ 50
CIFR Capacity	0.014635	≈ 50
TCIFR Capacity	0.015625	≈ 50

The analytical results have been evaluated using Mathematica software, while the simulation has been done by MATLAB using the Monte Carlo method. Based on the values in Table 2, it can be seen clearly that the simulation duration is still steady and significantly higher than that of the analytical expression. Thus, the analytic method remains the most optimal approach to evaluate the performance of each wireless communication system.

6 Conclusion

In this paper, various performance metrics employing an original and a close estimate PDF of the total of c.n.i.d Weibull RVs, including OP, ASER/ABER, and average capacities under various adaptation policies (ORA, OPRA, CIFR and TCIFR), are the results of approximate analytical expressions. The preciseness of obtained results has been verified using the Monte Carlo method. The MIMO-STBC shows evident usefulness in terms of performance and correlation; the phenomenon manifests a negative impact on the achievement of a wireless system of communication.

Abbreviations

MIMO	Multiple-input multiple-output
STBC	Space-time block codes
ASER	Average symbol error rate
MGF	Moment-generating function
ACC	Average channel capacity
PAM	Pulse-amplitude modulation
QAM	Quadrature amplitude modulation
i.n.i.d	Independent and not necessarily identically distributed
WFC	Weibull fading channels

Author contributions

All authors contributed to the study's conception and design. Material preparation, data collection, and analysis were performed by AB, YM, HB-A and FEB. The first draft of the manuscript was written by AB, and all authors commented on previous versions of the manuscript. All authors read and approved the final manuscript.

Funding

The authors declare that no funds, grants, or other support was received during the preparation of this manuscript.

Data availability

Data sharing is not applicable to this article as no datasets were generated or analyzed during the current study. Author on reasonable request.

Declarations

Competing interests

The authors have no relevant financial or non-financial interests to disclose.

Received: 17 November 2023 Accepted: 11 March 2024

Published online: 29 March 2024

References

1. S.M. Alamouti, A simple transmit diversity technique for wireless communications. *IEEE J. Sel. Areas Commun.* **16**(8), 656–715 (1998)
2. V. Tarokh, H. Jafarkhani, A.R. Calderbank, Space–time block codes from orthogonal designs. *IEEE Trans. Inf. Theory* **45**(5), 1456–1467 (1999)
3. G. Ganesan, P. Stoica, Space–time diversity using orthogonal and amicable orthogonal designs, in: *Proceedings of 2023 IEEE International Conference on Acoustics, Speech, & Signal Processing (ICASSP)*, Istanbul, Turkey, (2000)
4. S. Sandhu, A. Paulraj, Space–time block codes: a capacitive perspective. *IEEE Commun. Lett.* **4**(12), 384–386 (2000)
5. H. Shin, J.H. Lee, Performance analysis of space–time block codes over keyhole Nakagami- m fading channels. *IEEE Trans. Veh. Tech.* **53**(2), 351–362 (2004)
6. H. Zhang, T.A. Gulliver, Capacity and error probability analysis for orthogonal space–time block codes over fading channels. *IEEE Trans. on Wirel. Comm.* **4**(2), 808–819 (2005)
7. R. Gozali, B.D. Woerner, On the robustness of space-time block codes to spatial correlation, in: *IEEE Vehicular Technology Conference (VTC-S'02)* Birmingham, Germany, pp. 832–836, 6–9 May 2002.
8. A.E. Jorswieck, A. Sezgin, Impact of spatial correlation on the performance of orthogonal space–time block codes. *IEEE Commun. Lett.* **8**(1), 21–23 (2004)
9. A. Bessate, F. El Bouanani, A very tight approximate results of MRC receivers over independent Weibull fading channels. *Phys. Commun.* **21**, 30–40 (2016)
10. G. Femenias, BER performance of linear STBC from orthogonal designs over MIMO correlated Nakagami- m fading channels. *IEEE Trans. Veh. Technol.* **53**(2), 307–317 (2004)
11. M. Matthaiou, N.D. Chatzidiamantis, H.A. Suraweera, G.K. Karagiannidis, Performance analysis of space–time block codes over generalized- K fading MIMO channels, in: *IEEE Swedish Communication Technologies Workshop*, Stockholm, Sweden, pp. 68–73 (2011)
12. A. Maaref, S. Aissa, Capacity of space–time block codes in MIMO Rayleigh fading channels with adaptive transmission and estimation errors. *IEEE Trans. Wirel. Comm.* **4**(5), 2568–2578 (2005)
13. H. Zhang, T.A. Gulliver, Capacity and error probability analysis for orthogonal space-time block codes over fading channels. *IEEE Trans. Actions Wirel. Commun.* **4**(2), 808–819 (2005)
14. J. Perez, J. Ibanez, L. Vielva, I. Santamaria, Closed-form approximation for the outage capacity of orthogonal STBC. *IEEE Commun. Lett.* **9**(11), 961–963 (2005)
15. I.Y. Abualhaol, M.M. Matalgah, Capacity analysis of MIMO system over identically independent distributed Weibull fading channels, in: *IEEE International Conference on Communications (ICC)*, Glasgow, UK, 24–28 June 2007
16. A. Bessate, F. El Bouanani, A new performance results of MIMO system with orthogonal STBC over independent and identical Weibull fading channels, in: *Proceedings of International Conference on Advanced Communication Systems and Information Security (ACOSIS)*, Marrakech, Morocco, 17–19 Oct 2016
17. F. El Bouanani, A. Bessate, A comparative study on the performance of MIMO-STBC subject to Weibull fading channels. *Int. J. Commun. Syst.* **31**(13), e3731 (2018)
18. F. El Bouanani, D.B. da Costa, Accurate closed-form approximations for the sum of correlated Weibull random variables. *IEEE Wirel. Commun. Lett.* **7**(4), 498–501 (2018)
19. S. Sandhu, A. Paulraj, Space time block codes: a capacitive perspective. *IEEE Commun. Lett.* **4**(12), 384–386 (2000)
20. X. Deng, W. Zhang, C. Tellambura, Amount of fading analysis for transmit antenna selection in MIMO systems, in: *Proceedings of the Wireless Communications and Networking Conference (WCNC'07)*, (2007), pp. 1161–1165, Hong Kong
21. M. Lupupa, M.E. Dlodlo, Performance analysis of transmit antenna selection in Weibull fading channel, in: *Proceedings of AFRICON'09*, pp. 1–6 (2009), Nairobi, Kenya
22. G.K. Karagiannidis et al., Equal-gain and maximal-ratio combining over nonidentical Weibull fading channels. *IEEE Trans. Wirel. Commun.* **4**(3), 841–846 (2005)
23. M. Abramowitz, I.A. Stegun, *Handbook of Mathematical Functions with Formulas, Graphs, and Mathematical Tables* (Dover, New York, 1972)
24. J. Cheng, C. Tellambura, N.C. Beaulieu, Performance analysis of digital modulations on Weibull fading channels, in: *Proceedings of IEEE Vehicular Technology Conference (VTC'38)*, pp. 236–240, (2003), Grenoble, France
25. A.J. Goldsmith, P.P. Varaiya, Capacity of fading channels with channel side information. *IEEE Trans. Inf. Theory* **43**(6), 1986–1992 (1997)
26. I.W. Research, *Mathematica*, version 13.2, Champaign, IL, (2022), [Online] Available: <http://functions.wolfram.com/>
27. M. Abramowitz, I.A. Stegun, *Handbook of mathematical functions with formula, graphs, and mathematical tables*, National Bureau of Standards, Applied Mathematical Series 55, (1964)

Publisher's Note

Springer Nature remains neutral with regard to jurisdictional claims in published maps and institutional affiliations.